

ChemComm

Accepted Manuscript



This is an *Accepted Manuscript*, which has been through the Royal Society of Chemistry peer review process and has been accepted for publication.

Accepted Manuscripts are published online shortly after acceptance, before technical editing, formatting and proof reading. Using this free service, authors can make their results available to the community, in citable form, before we publish the edited article. We will replace this *Accepted Manuscript* with the edited and formatted *Advance Article* as soon as it is available.

You can find more information about *Accepted Manuscripts* in the [Information for Authors](#).

Please note that technical editing may introduce minor changes to the text and/or graphics, which may alter content. The journal's standard [Terms & Conditions](#) and the [Ethical guidelines](#) still apply. In no event shall the Royal Society of Chemistry be held responsible for any errors or omissions in this *Accepted Manuscript* or any consequences arising from the use of any information it contains.



www.rsc.org/chemcomm

The insulin degrading enzyme activates ubiquitin and promotes the formation of K48 and K63 diubiquitin.

Received 00th January 20xx,
Accepted 00th January 20xx

G. Grasso,^a V. Lanza,^b G. Malgieri,^c R. Fattorusso,^c A. Pietropaolo,^d E. Rizzarelli^{a,b} and D. Milardi^{*b}

DOI: 10.1039/x0xx00000x

www.rsc.org/

Abstract. We report an ATP-dependent ubiquitin conjugation with IDE which, in turn, promotes Ub-Ub linkages in tube tests. We propose a novel function for IDE as a non-canonical ubiquitin activating enzyme.

The insulin-degrading enzyme (IDE) is a ubiquitous zinc metalloprotease that is generally considered to be crucial in controlling insulin degradation.¹ However, the role played by IDE in this proteolytic pathway is still a subject of some controversy,² and an increasingly large number of evidences point to a broader physiological role for this metalloenzyme. For example IDE is present in tissues, such as testis, that are not involved in insulin metabolism.³ Furthermore, although IDE is mainly located in the cytosol, it has also been found in peroxisomes where it exerts specific proteolytic activities.⁴ In neurons, IDE is also present at the membrane surface and can be delivered to the extracellular space.^{5,6} A number of evidences suggest that extracellular IDE is a key regulator of amyloid levels and its inhibition/malfunction has been proposed to be implicated in the pathogenesis of Alzheimer's disease and type 2 diabetes mellitus.⁷⁻¹² Cytosolic IDE is also involved in the cleavage of the intracellular domain of the β -amyloid precursor protein (APP) that is activated to regulate the transcriptional activity in the nucleus.^{13,14} It has been also evidenced that IDE is associated in the cell to the 26S proteasome, the endpoint of the ubiquitin-proteasome system (UPS).¹⁵ Additionally, ubiquitin (Ub) was shown to inhibit insulin degradation by IDE and alter insulin-IDE

interactions.^{16,17} It is controversial whether Ub itself may be degraded by IDE.^{17,18} Two recent studies have demonstrated that IDE silencing induces a reduction of the levels of ubiquitinated proteins^{19,20} and one possible explanation of this could involve the inhibition of the proteasome by IDE.¹⁹ However, to date, little is known about the exact role(s) played by IDE in regulating the UPS. The UPS takes advantage of Ub to regulate the intracellular fate of proteins via numerous biological processes including proteasomal degradation or autophagy.^{21,22} At the apex of the UPS there is an activating enzyme (E1) which, in the presence of Mg^{2+} and ATP, binds Ub and then drives the activated Ub-E1 thioester-bonded complex to downstream Ub conjugation routes.²³ Ub-tagged proteins are substrates for the conjugation of further Ub moieties by Ub conjugating enzymes (E2s), leading to the formation of differently arranged polyubiquitin chains which, in turn, provide dainty specificity in multifunctional Ub signaling.²³ In the last two decades, an article of faith in the field was that a unique E1 enzyme, UBA1, may bind to and activate Ub. Nevertheless, recent reports that distinguished at least eight E1 enzymes in humans have confuted this dogma and opened new avenues in the research focusing on alternative Ub activation routes.²⁴ In particular, these studies have evidenced that, although E1s may have rather different structures, two bacterial proteins, MoeB and ThiF, are highly homologous to a domain shared by all E1s that drives Ub binding and adenylation.²⁵

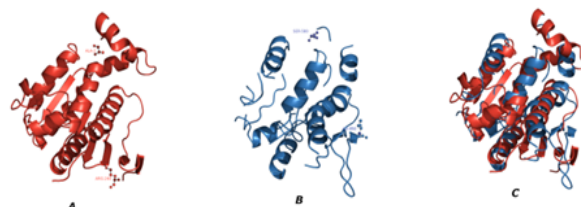


Figure 1. 3D representations of MoeB (pdb code: 1JWA) (a), the Ser580-Ile850 domain of IDE (pdb code: 2JG4) (b) and their superimposition of the two aligned structures (c). The 3D structures were superimposed by using the jFATCAT alignment tool of the protein databank website.

^a Dipartimento di Scienze Chimiche, Università degli Studi di Catania, V.le A. Doria 6, 95125, Catania, Italy.

^b Istituto di Biostrutture e Bioimmagini, Consiglio Nazionale delle Ricerche, Via P. Gaifami 18, 95126 Catania, Italy. E-mail: danilo.milardi@cnr.it

^c Dipartimento di Scienze e Tecnologie Ambientali Biologiche e Farmaceutiche, Seconda Università degli Studi di Napoli, Via Vivaldi 43, 81100 Caserta, Italy.

^d Dipartimento di Scienze della Salute, Università degli Studi Magna Graecia di Catanzaro, Viale Europa - 88100 - Catanzaro, Italy.

Electronic Supplementary Information (ESI) available: materials and methods, alignment of IDE with MoeB, SPR sensograms, NMR contact maps, western blots. See DOI: 10.1039/x0xx00000x

Thus, the presence of a Moeb/ThiF domain in a protein may somehow represent a signature for a possible E1-like activity of the protein. The observed structural similarities existing between the Moeb-like domain of UBA1 and the C-terminal region of IDE, (Fig. 1 and Scheme S1, Fig. S1 and S2 of Supplementary Info) encouraged us to investigate the possible involvement of IDE in activating the ubiquitination pathway. A prerequisite for such a study is a thorough description of stoichiometry, binding equilibrium and residues involved in IDE/Ub interactions. Surface Plasmon Resonance (SPR) sensograms describing the interaction between immobilized IDE and Ub flowing above the SPR chip surface evidenced a binding affinity similar to that of other IDE substrates²⁶ even in the presence of EDTA, a strong inhibitor of the peptidase activity of IDE (see Fig S3 and Table S1 of Supplementary info). Notably, although the presence of EDTA and the consequent chelation of the Zn²⁺ ion in the catalytic site of the enzyme lowers the Ub affinity for IDE by changing the dissociation rate constant k_d , IDE is still able to bind Ub even when its proteolytic activity is turned off. The ¹H, ¹⁵N, chemical shift perturbation NMR analysis of Ub after sub-stoichiometric addition of IDE shows that the overall protein fold is maintained, even though a number of resonances were perturbed. To quantify these changes, intensity variations of the amide cross-peaks in the presence and absence of IDE (ΔI) were determined and plotted versus the residue number (Fig.2). Mapping these differences onto the structure (Fig. S4 of Supplementary Info) outlines a region of Ub interaction involving residues G2, F4, L15, I44, F45, D52, V70, R72, R74. Of note, these residues resemble the intermolecular contacts driving canonical E1-Ub interactions which mainly involve two Ub domains i.e. the hydrophobic patch centred around Ile44 and Val70 and the Ub C-terminus.²⁷ In order to describe the atomistic details of IDE-Ub interactions, NMR results were refined by molecular modeling. Upon docking IDE with Ub, three main binding poses have been evidenced. In all of them, in accordance with the SPR results, the Ub anchoring site to IDE is far from the enzyme catalytic site. Indeed, Ub features the R74 residue located in the C-terminal segment as its anchoring site (Figure 3). In particular, in the first binding pose, R74 of Ub contacts through salt-bridge interactions the E529 residue of IDE (Figure 3a).

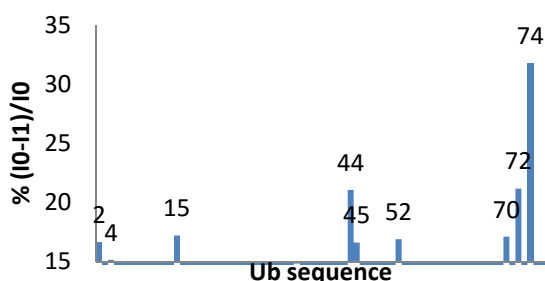


Figure 2. Human Ub intensity variations of the ¹H and ¹⁵N amide cross-peaks after addition of IDE as a function of protein residue numbers. ¹⁵N-¹³C labeled Ub (100 μM) and unlabeled IDE (10 μM) were dissolved in 550 μL of 50 mM phosphate buffer pH 7 and 10% D₂O. Further experimental details are reported in the supplementary information.

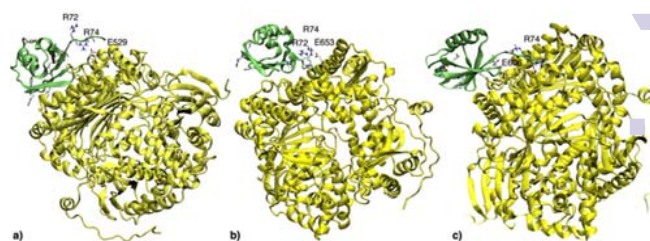


Figure 3. The three lowest energy binding poses for the IDE/Ub complex. IDE sections are shown by yellow ribbons, Ub sections are shown by green ribbons. The residues of Ub interacting with IDE are shown by solid sticks and those involved in salt-bridge interactions are also labeled. Docking simulations have been performed using HADDOCK interface. The starting coordinates of Ub were considered from the X-ray structure of the complex between the UBA1 enzyme and Ub (pdb code: 3CMM). The residues Q2, F4, L15, I44, F45, D52, V70, R72, R74 of Ub were considered as active residues, since observed through NMR experiments to interact with IDE. Structures underwent rigid body energy minimization, semirigid simulated annealing in torsion angle space, with a final clusterization of the results.

In this pose, the flexible C-terminal tail of Ub approaches the flexible segment of IDE comprising A516 to Y547. A second binding pose involves R74 and R72 of Ub both contacting E653 of IDE (Figure 3b), while IDE is rotated through the vertical axis. In this pose, the flexible C-terminal tail of Ub approaches the loop connecting the alpha-helix comprising Q638 to M647 and the alpha-helix encompassing E656 to N671. A third binding pose features Ub rotated through the horizontal axis. Here, R74 of Ub contacts the E606 residue of IDE through salt-bridge interaction (Figure 3c). In this pose, the flexible C-terminal tail of Ub faces the short loop encompassing E606 and connecting the long alpha helix belonging to L588 towards E612.

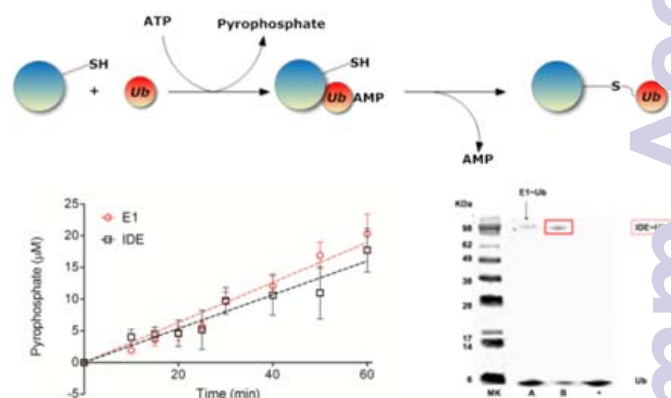


Figure 4 Upper panel. Reaction scheme of Ub activation. Bottom left panel. Pyrophosphate formation during Ub activation by IDE (open black squares) and by E1 (open red circles) in the presence of the E2 25K conjugating enzyme was monitored by colorimetric assay at $\lambda=720$ nm with a time interval of 5 minutes by a 96 well plate reader Varioskan. In each well, 10 μL of a 400 mM EDTA solution were used to quench all reactions. Then, solutions were incubated for 10 min with 200 μL of 3 mM ammonium molybdate in 0.6 M HCl (60% AcN/W). The colorimetric reaction was started by adding 80 μL of a solution of ascorbic acid (500 mM) in 2M HCl (60% AcN/W). Reaction mixture contained 1 μM E2 25K, 0.5 μM UBA1, 15 μM Ub (data points are an average of three independent measurements and the error bars are the standard deviation of the experiments). Bottom, right panel. Western Blots revealing the formation of a thioester linkage between IDE and Ub (see suppl. Information). The monitoring of formation of activated ester covalent linkage between Ub and E1 and IDE, using the

ubiquitylation kit ABCAM (139472). Lane A: Ub (50 μ M), E1 (2.5 μ M), IPP (10 U/ml), DTT (1mM), MgATP (5 mM) in ubiquitinylation buffer (Tris 50 Mm pH 7,2); lane B: Ub (50 μ M), IDE (2.5 μ M), inorganic pyrophosphatase (IPP) (10 U/ml), DTT (1 mM), MgATP (5 mM) in ubiquitinylation buffer (Tris 50 mM pH 7,2); control - : same conditions as for lane B without ATP.

From the former poses, R74 results the first recognition site of Ub that in turn causes the movement of V70 and R72, accompanied by the movement of the central region (I44, F45, D52) and followed by the Ub N-terminal region (Q2, F4, L15). Remarkably, in all the three binding poses, Ub binds MoeB-like domains of IDE thus resembling the behavior of a Ub-activating enzyme. Normally, the E1 enzyme binds ATP-Mg²⁺ and Ub and catalyses acyl adenylation of the Ub C-terminus with concomitant release of pyrophosphate. Next, a cysteine of the E1 enzyme attacks the Ub-AMP complex through acyl substitution, creating a high energy Ub-E1 thioester bond (see the upper panel of Fig. 4). Therefore, in order to establish if IDE may act as an E1 we employed a colorimetric assay to monitor the amount of pyrophosphate released during IDE- (or E1-) mediated ubiquitin activation (see bottom left panel of Fig. 4).²⁸ These results evidence that, in the presence of Mg²⁺, DTT and Ub, IDE consumes ATP at approximately the same rate as E1. Furthermore, the E1-Ub covalent complex should be visible if Ub activation works properly. To show to what extent IDE may mimic E1, we have incubated Ub and IDE (or E1) in activation buffer (MOPS, Mg²⁺, ATP, DTT), (bottom right panel of Fig. 3). The Western blot analysis confirms that the formation of the E1-Ub complex has only occurred in the presence of ATP (bottom right panel of Fig. 4, line B). Next, we investigated whether IDE may replace E1 in promoting Ub chain growth. To this aim, western blotting assays were performed to assess the impact of IDE on K48 and K63 self-polyubiquitination reactions in tube tests as reported elsewhere.^{29,30} Indeed, if IDE is used in place of E1 to promote K48 and K63 Ub chain growth, only the formation of Ub2 species is observed (Fig. 5). On the contrary, if we use IDE in place of E2, Ub chain elongation reactions cannot take place (Figure S5 of Supplementary info). It is likely that IDE-activated ubiquitin units may self-conjugate to produce also K6, K11 or other forms of polymeric chains. Unfortunately, it is difficult to verify this hypothesis in tube tests because cell-free protocols for these self-conjugation reactions have not yet been optimized.³¹ In conclusion, we identify at least three IDE-Ub binding modes. None of them involve the proteolytic site of IDE. By contrast, Ub binds a region of IDE which is structurally analogous to a domain that is common to all Ub-activating enzymes.

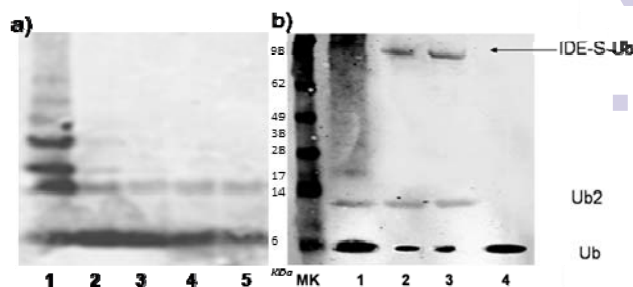


Figure 5. Western blots showing that IDE is a E1 Ub activating enzyme in K63- (a) and K48 (b) self-polyubiquitination reactions. Panel a) line1: Ub (5 μ M), E1(UBA1) (100nM), DTT (500 μ M), MgATP (5 mM) UbCH1 (500nM) MMS2 (500nM) in ubiquitinylation buffer (MOPS 50 Mm pH 7,2); lines 2,3,4,5: same than line 1 with different concentrations of IDE (1,3, 5,10 μ M) instead of UBA1. Panel b) line1: Ub (10 μ M), UBA1 (500nM), DTT (500 μ M), MgATP (5 mM) E225K (1 μ M) in ubiquitinylation buffer (MOPS 50 Mm pH 7,2); lanes 2, 3: Ub (10 μ M), DTT (500 μ M), MgATP (5 mM) E225K(1 μ M) in ubiquitinylation buffer (MOPS 50 Mm pH 7,2) with different concentrations of IDE (1,10 μ M) instead of E1; lane 4 control - : as in lane 2 without ATP. Samples were analyzed as described in the caption of figure 4 and in supplementary info.

Moreover, IDE forms an IDE-Ub adduct in a ATP-dependent fashion and is, in turn, able to promote the formation of K48 and K63 diubiquitin in the presence of E2 conjugating enzymes. It is worthy to remind here that unanchored diubiquitin chains are widely expressed in mammalian cells and represent biologically relevant species³² that may be transferred en bloc to rapidly promote Ub-mediated signaling.³³ For example, K48-diubiquitin was found to be a competitive inhibitor of the 26S proteasome.³⁴ In addition, K48 and K63 ubiquitin dimers have been shown to regulate in vivo the activity of specific Ub-processing proteases, the Ub carboxyl-terminal hydrolases (UCHs).³⁵

It is challenging to fully describe, on a structural basis, the mechanism of E1-like function of IDE and some key processes including IDE conformational changes during thioester formation, IDE-E2 interactions during transthioesterification and IDE-mediated formation of Ub-Ub isopeptide linkage, remain unknown. Our results evidence a Ub-activating activity of IDE in cell-free polyubiquitination models and open avenues to further studies addressing the cross-talk between IDE and Ub-dependent protein quality control machinery in ensuring proteome integrity. This work was supported by the Italian Ministry of University and Research (MIUR), Prin n° 2010M2JARJ.

References

- 1 A.B. Becker, R.A. Roth, *Methods Enzymol.* 1995, **248**, 693-703.
- 2 J.P. Maianti, A. McFedries, Z.H. Foda, R.E. Kleiner, X.Q. Du, M.A. Leissring, W.J. Tang, M.J. Charron, M.A. Seeliger, A. Saghatelian, D.R. Liu, *Nature*, 2014, **511**(7507), 94-U474.
- 3 W.L. Kuo, A.G. Montag, M.R. Rosner, *Endocrinology* 1993, **132**, 604-611.
- 4 W.L. Kuo, B.D. Gehm, M.R. Rosner, W.Li, G.Keller, *J. Biol. Chem.* 1994, **269**, 22599-22606.

- 5 K.A. Seta, R.A. Roth, *Biochem. Biophys. Res. Commun.* 1997, **231**, 167-171.
- 6 K. Vekrellis, Z. Ye, W.Q. Qiu, D.M. Walsh, D. Hartley, V. Chesneau, *J. Neurosci.* 2000, **20**, 1657-1665.
- 7 W.Q. Qiu, D.M. Walsh, Z. Ye, K. Vekrellis, J. Zhang, M.B. Podlisky, M.R. Rosner, A. Safavi, L.B. Hersh, D.J. Selkoe, *J. Biol. Chem.* 1998 **273**, 32730-32738.
- 8 I.V. Kurochkin, S. Goto, *FEBS Lett.* 1994, **345**, 33-37;
- 9 W. Farris, S. Mansourian, Y. Chang, L. Lindsley, E.A. Eckman, M.P. Frosch, C.B. Eckman, R.E. Tanzi, D.J. Selkoe, S. Guenette, *Proc. Natl Acad. Sci. USA*, 2003, **100**, 4162-4167.
- 10 J.R. McDermott, A.M. Gibson, *Neurochem. Res.* 1997, **22**, 49-56.
- 11 Q. Guo, M. Manolopoulou, Y. Bian, A. B. Schilling, W.J. Tang, *J. Mol. Biol.* 2010, **395**, 430-443.
- 12 N. Rudovich, O. Pivovarova, O. Fisher, A. Fischer-Rosinsky, J. Spranger, M. Möhlig, M. B. Schulze, H. Boeing, A.F. Pfeiffer, *J. Mol. Med.* 2009, **87**, 1145-1151.
- 13 D. Edbauer, M. Willem, S. Lammich, H. Steiner, C. Haass, *J. Biol. Chem.* 2002, **277**, 13389-13393.
- 14 G. Pandini, V. Pace, A. Copani, S. Squatrito, D. Milardi, R. Vigneri, *Endocrinology*, 2013, **154**, 375-387.
- 15 W.C. Duckworth, R.G. Bennett, F.G. Hamel, *J. Biol. Chem.* 1994, **269**, 24575-24580.
- 16 T. Saric, D. Müller, H.J. Seitz, K. Pavelic *Mol. Cell. Endocrinol.* 2003, **204**, 11-20.
- 17 G. Grasso, E. Rizzarelli, G. Spoto, *Biochim. Biophys. Acta* 2008, **1784**, 1122-1126.
- 18 L. A. Ralat, V. Kalas, Z. Zheng, D. Goldman, T. RR. Sosnick, W. J. Tang, *J. Mol. Biol.* 2011 **406**, 454-466.
- 19 G.R. Tundo, D. Sbardella, C. Ciaccio, A. Bianculli, A. Orlandi, M. G. Desimio, G. Arcuri, M. Coletta, S. Marini, *J. Biol. Chem.* 2013, **288**, 2281-2289.
- 20 D. Sbardella, G.R. Tundo, F. Sciandra, M. Bozzi, M. Gioia, C. Ciaccio, U. Tarantino, A. Brancaccio, M. Coletta, S. Marini, *PLoS One* 2015, **10**: e0132455.
- 21 A. Hershko, H. Heller, S. Elias, A. Ciechanover *J. Biol. Chem.* 1983, **258**, 8206-8214.
- 22 D. Milardi, F. Arnesano, G. Grasso, A. Magri, G. Tabbi, S. Scintilla, G. Natile, *Angew. Chem. Int. Ed.* 2007, **119**, 8139-8141.
- 23 B. A. Schulman, J. W. Harper. *Nat. Rev. Mol. Cell Biol.* 2009, **10**, 319-33.
- 24 A. Hershko, A. Ciechanover, *Annu. Rev. Biochem.* 1992, **61**, 761-807.
- 25 A. M. Burroughs, M. I. Lakshminarayan, L. Aravind, *Proteins* 2008, **75**, 895-910
- 26 G. Grasso, C. Satriano, D. Milardi, *Biophys. Chem.* 2015, **203-204**, 33-40.
- 27 I. Lee, H. Schindelin, *Cell* 2008, **134**, 268-278.
- 28 C. E. Berndsen, C. Wolberger, *Anal Biochem.* 2011, **418**, 102-110.
- 29 G. Arena, F. Bellia, G. Frasca, G. Grasso, V. Lanza, E. Rizzarelli, G. Tabbi, V. Zito, D. Milardi, *Inorg. Chem.* 2013, **52**, 9567-9573.
- 30 G. Arena, R. Fattorusso, G. Grasso, G. I. Grasso, C. Isernia, G. Malgieri, D. Milardi, E. Rizzarelli, *Chem. Eur. J.* 2011, **17**, 11596 - 11603.
- 31 K. C. Dong, E. Helgason, C. Yu, L. Phu, D. P. Arnott, I. Bosanac, D. M. Compaan, O. W. Huang, A. V. Fedorova, D. S. Kirkpatrick, S. G. Hymowitz, E. C. Dueber, *Structure* 2011, **19**, 1053-1063.
- 32 J. Strachan, L. Roach, K. Sokratous, D. Tooth, J. Long, T.P. Garner, M. S. Searle, N. J. Oldham, R. Layfield, *J. Proteome Res.* 2012, **11**, 1969-1980.
- 33 M. Hochstrasser, *Cell* 2006, **124**, 27-34.
- 34 J. Piotrowski, R. Bear, L. Hoffman, K. D. Wilkinson, R. E. Cohen, C. M. Pickart, *J. Biol. Chem.* 1997, **272**, 23712-23721.
- 35 R. Setsuie, M. Sakurai, Y. Sakaguchi, K. Wada, *Neurochem. Int.* 2009, **54**, 314-321.